Faculty of Science

2D plain strain, pure shear deformation experiments in ice – Preparation of strain gauges teaching material for undergraduate students

Elias Waltenburg Thurell

Degree of Bachelor of Science
with a major in Earth Sciences
15 hec

Department of Earth Sciences
University of Gothenburg
2020 B-1094

UNIVERSITY OF GOTHENBURG

UNIVERSITY OF GOTHENBURG
Department of Earth Sciences
Geovetarcentrum/Earth Science Centre

2D plain strain, pure shear deformation experiments in ice – Preparation of strain gauges teaching material for undergraduate students

Elias Waltenburg Thurell

ISSN 1400-3821

B1094
Bachelor of Science thesis
Göteborg 2020

Mailing address
Geovetarcentrum
S 405 30 Göteborg

Address
Geovetarcentrum
Guldhedsgatan 5A

Telephone
031-786 19 56

Geovetarcentrum
Göteborg University
S-405 30 Göteborg
SWEDEN

Abstract

In this report I explore the viability of using an ice thin section with carbon dioxide inclusions as a material for students to practice the Fry- and R_f/Φ strain analysis methods. The use of this material allows the students to follow the deformation process from the initial to the final stages in incremental steps, something which more conventionally used materials, such as conglomerates and ooids will not allow.

The analysis presented in this report was done by producing and deforming an ice thin section in a laboratory environment, which allowed for in situ observation of all intermediate stages of deformation. The deformation process was recorded using a fabric analyzer. A total of 16 microphotographs were analyzed using the EllipseFit freeware software, by tracing all bubble inclusions present in the images, excluding obvious outliers.

The analysis show that the final and all intermediary incremental strain of an ice thin section sample can be calculated and tracked using the Fry- and R_f/Φ strain analysis methods.

I supplemented this report with practical examples of student exercises, one which teaches manual application of the methods and one which teaches the software-based application of the methods.

Table of Contents

1 Introduction

There are several tools students in structural geology students need to be acquainted with at an early stage of their education. These tools include the Fry method and the R_f/Φ method, which are used to measure the accumulated strain a section of rock has undergone during one or several deformation stages (Soares & Dias, 2015). Typically, these methods are taught by having the students measure and analyze either pictures or samples of deformed rocks with marker-objects which had a spherical or spheroid shape in the initial stages of deformation. Any elongation and reorientation of these markers during the deformation process is, in theory, equal to the elongation and reorientation of the rock fabric (Twiss & Moores, 1992).

In studying the structures and microstructures of rocks, the history of deformation is often lost as the creep of rock fabric during deformation is nearly impossible to follow in incremental stages (C. J. L. Wilson, Peternell, Piazolo, & Luzin, 2012). When students are doing their exercises, they typically do measurements on a sample in its final stage of a long deformation process. To show the progressive deformation of a crystalline material in detail, a different material which allows continuous observations during deformation is needed. One such material which serves as a good analogue for mid- to lower crustal rock textures is ice (C. J. L. Wilson et al., 2012).

The aim of this thesis is to exemplify the use of plane strain and pure shear progressively deformed ice thin sections with air bubble inclusions as a teaching material for undergrad student. This is done by constructing a student exercise using images depicting an ice thin section during several stages of deformation. The student exercise will focus on teaching the Fry and the R_f/Φ methods. It also serves to evaluate if ice with gaseous inclusions is a viable medium for testing and teaching the proposed methods.

1.1 The R_f/Φ method

This technique for analyzing strain was first described in 1967 by John G. Ramsay (Ramsay, 1967), and later refined by several authors (Dunnet, 1969; Matthews, Bond, & Van Den Berg, 1974; Shimamoto & Ikeda, 1976). It is probably the most widely used method for analyzing strain in rocks (Lisle, 1985). The method is based the measurement of a group of elliptical markers in a sample and involves two variables. The first variable is called R_f, the final ratio between the long and the short axis of an elliptical marker, which is a measure of elongation. The second variable, Φ (“phi”), is a measurement of the deviation of the major axis orientation from the strain X direction (mainly the deformation related lineation) in the sample.

The most common technique used to evaluate the finite strain from R_f- and Φ-values is to plot the values on a Cartesian plot (Fig 1) to find the minimum and maximum R_f-values. The R_f-values may then be used to calculate the Axial ratio of both the final and initial strain ellipse (R_s and R_i). This technique hinges on the fact that the initial orientation and ellipticity of a marker object will influence its final ellipticity and orientation (Twiss & Moores, 1992).

An elliptical marker which is aligned parallel to the strain X direction will increase its ellipticity (R_f) in proportion to the strain imposed on the sample (see object b in fig 1). This is the maximum increase possible in the sample and thus this marker represents the maximum R_f-value possible out of a sample ($R_{f(max)}$) and is proportional to both the initial strain and the final strain ($R_{f(max)} = R_i \times R_s$). A marker aligned parallel to the maximum shortening direction, which is perpendicular to the strain X direction, will experience a shortening, thus exhibiting the lowest R_f-value after deformation ($R_{f(min)}$) (see object c in figure 1). It is also directly proportional to the initial and imposed strain on the sample, albeit

inversely to the $R_{f(max)}$: ($R_{f(min)}$= R_s/R_i) (Twiss & Moores, 1992). These relationships are visualized in figure 1.

For the relationships and the strain ratio relationships to be viable, the initial distribution of long axis orientations is assumed to be randomly distributed. Deviations from an initially random orientation compromises the reliability of the method (Lisle, 1985).

An underlying assumption when using the method is that the objects chosen for study will behave as passive markers during deformation. This is key if they are to represent the bulk finite strain of the sample. All versions of the method assume optimal conditions where the properties of the matrix and marker does not differ significantly (Vitale & Mazzoli, 2005).

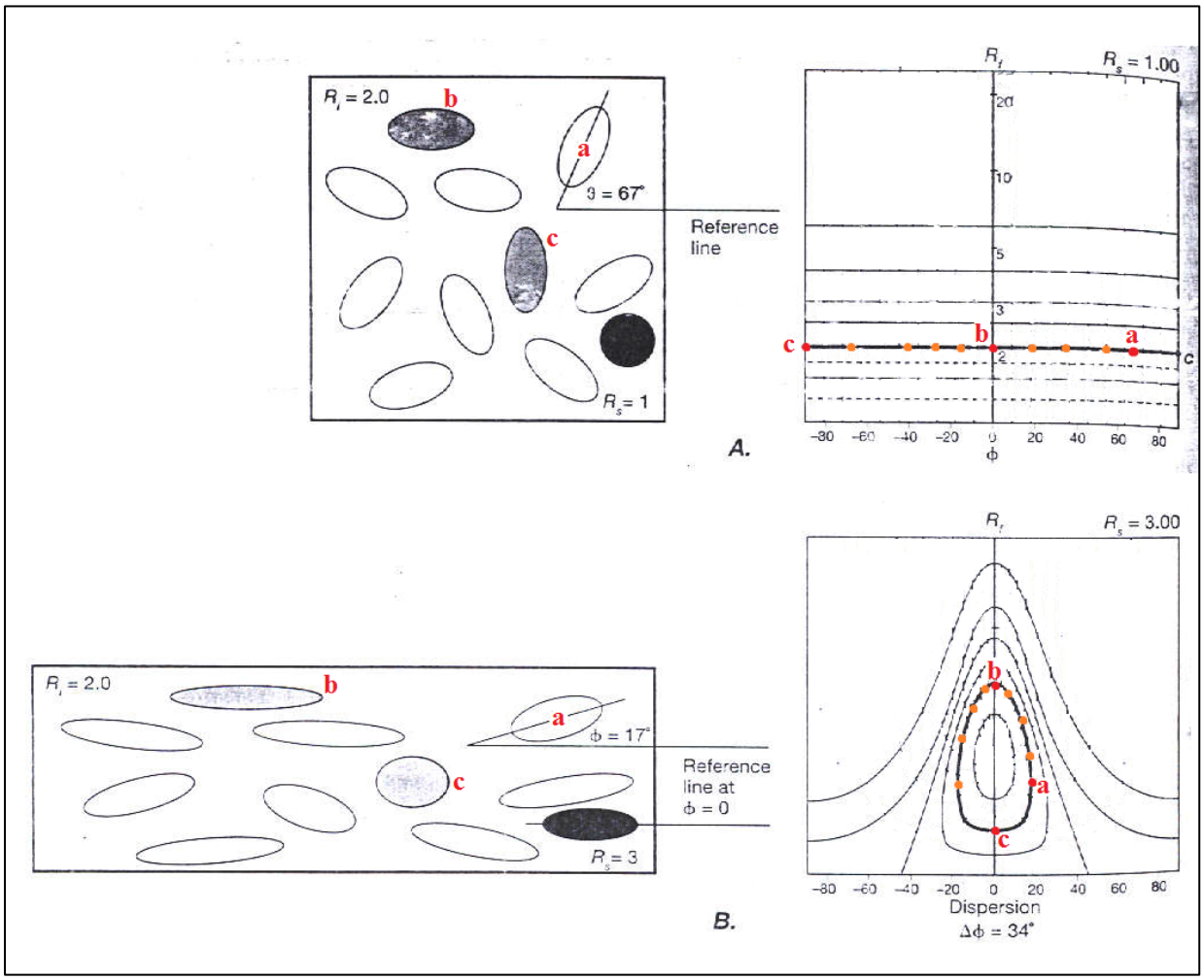

*Figure 1: The R_f/Φ method applied on a sample with objects which all have identical initial axial ratios. The reference line is parallel to the line of maximum elongation in the sample. Notice how the objects response depend on their initial orientation. A) The sample before deformation. As all ellipses have identical axial ratios, they project along one line on the plot. Object **a**) is aligned in a random orientation, object **b** is aligned parallel to the direction of maximum strain, object **c**) is aligned perpendicular to the direction of maximum strain. B) The sample after deformation. The objects have experience different degrees of elongation due to different initial long axis orientations. Object **b** and **c** have received the most and the least increase to their ellipticity respectively. Object **a**, along with all other objects (orange dots on the plot) exhibit intermediary increases to their ellipticity. We see that the final ellipticity of the object **b** (R_{fmax}) is directly dependent on its initial ellipticity (R_i) and the full effect of the imposed strain (R_s), a relationship which is written as $R_{fmax}=R_i X R_s$. Conversely for object **c** (R_{fmin}) its initial ellipticity opposes the strain imposed on the marker (R_s), a relationship which is written as $R_{fmin}=R_s / R_i$.*
Modified from Twiss & Moores, (1992).

1.2 The Fry method

The Fry method (Fry, 1979) is a way to analyze center-to-center measurements of objects in a matrix and produce a strain analysis. It involves plotting the distances and directions between individual markers as points on a paper. A typical method involves overlaying a picture of a deformed sample with a sheet of tracer film, repeatedly centering it over an object and plotting the centers of its immediate neighbors. It is assumed that the distances between the centers of objects in an undeformed state is uniform. If this is true, then the distances between the object centers in a deformed state provides a measure of the bulk strain the sample has been subjected to (Twiss & Moores, 1992). By repeatedly plotting the distances and directions between the object centers, a central void will emerge in the center of the paper. This 'central void' represents the final strain ellipse of the measured sample. Figure 2 shows the application of the method. Notice how the strain ellipse (Fig 2B) is represented by the central void defined by the projected object centers in the final overlay (Fig 2E).

This type of plot is called a Fry plot and is one of the most common strain-analysis tools used today (Yamaji, 2005).

Analogue interpretations of Fry plots are somewhat subjective as the central void is typically traced by hand and observers may judge the shape of the central void differently. In order to produce more objective interpretations, computerized methods which have been developed define the edges of the central vacancy and calculate the projected ellipse (Waldron & Wallace, 2007).

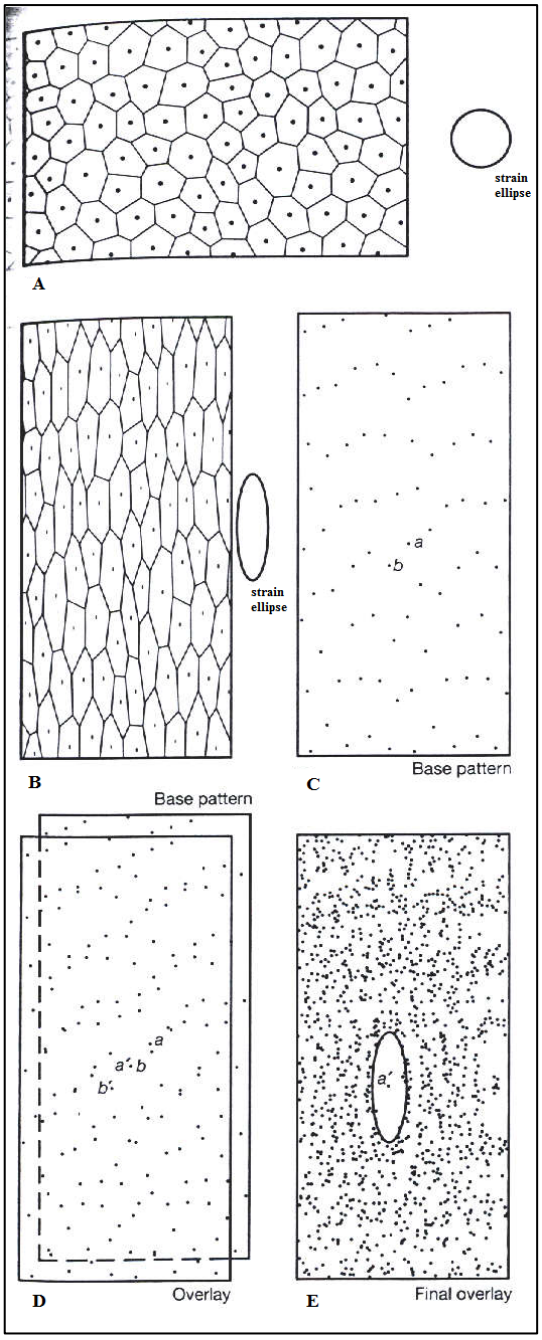

*Figure 2: A graphical representation of how the Fry method is performed. A) a sample in an undeformed state with its corresponding strain ellipse. B) The same sample in a deformed state with its corresponding strain ellipse. C) a sheet containing all center points of the sample. D) a separate sheet with a reference point (a´) and all point transcribed from when the reference point was superimposed over point **a**. The reference point is now superimposed over the center point of object **b** as projected on the on the base pattern. E) The result when all center points have been projected onto the paper. Modified from Twiss & Moores, (1992)*

1.3 Ice as an analogue for rocks

Linking microstructural evolution with rheology has proven problematic in geological material, i.e. rocks, due to the high pressures and temperatures needed to recreate the natural conditions of rock creep (C. J. L. Wilson et al., 2012). For practical reasons this limits our observations to initial and final characteristics of the samples. Because of this a continuous observation of microstructure evolution is not possible and an analogue material, suitable to study under more favorable conditions, is needed if we want to study the relationship between stress and strain in high detail. Ice has proven a very good analogue in this regard and its low melting point allows it to deform under conditions where the

progression of deformation can be continuously recorded(C. J. L. Wilson, Peternell, Piazolo, & Luzin, 2014).

Two-dimensional in situ plane strain, pure shear and simple shear deformation experiments of ice allow direct observation of crystal response to imposed strain. The process may be automated with the use of an automated fabric analyzer (Peternell, Russell-Head, & Wilson, 2011). It involves placing a thin, around 250 µm thick, sample between opposing flat blades made of stainless steel which are connected to anvils which closes by converging at equal rate (Fig 3). These converging anvils will be imposing constant pressure on the sample, driven by a small motor. The sample is also restrained between two layers of silicone grease and glass plates which prohibit lateral extension during deformation. The motor gives a constant speed which in turn allows for a constant closing rate of the blades. Experiments on ice may be carried out in ambient temperatures of 10 ± 2 degrees Celsius (Peternell et al., 2011).

2 Method

2.1 Ice thin section data

The purpose of these experiments was to produce a series of data frames recording the progressive deformation of an ice matrix with clear strain markers. To produce clear markers, carbonated water was frozen which produced an ice matrix with high bubble inclusion density.

The sample was prepared by cutting an about 70x40x20 mm rectangular portion from the carbonated water ice core. To level the analyzed surface, it was ground with an abrasive paper and frozen to one of the glasses of the deformation press. The sample was then shaved to a thickness of 250 micrometers using microtome thinning and then the shaved side was polished with abrasive paper. After this the sample was cut to its final dimensions of about 50x30 mm.

To minimize possible friction the sample was then floated on the glass by warming it from underneath and placed between two new glass plates which were lubricated with silicone oil.

It was then subjected to a constant shortening, imposing a plane strain, pure shear by placing it between the converging anvils of the deformation press and using the machine as detailed above (fig 3a). deformation press) (Peternell et al., 2011).

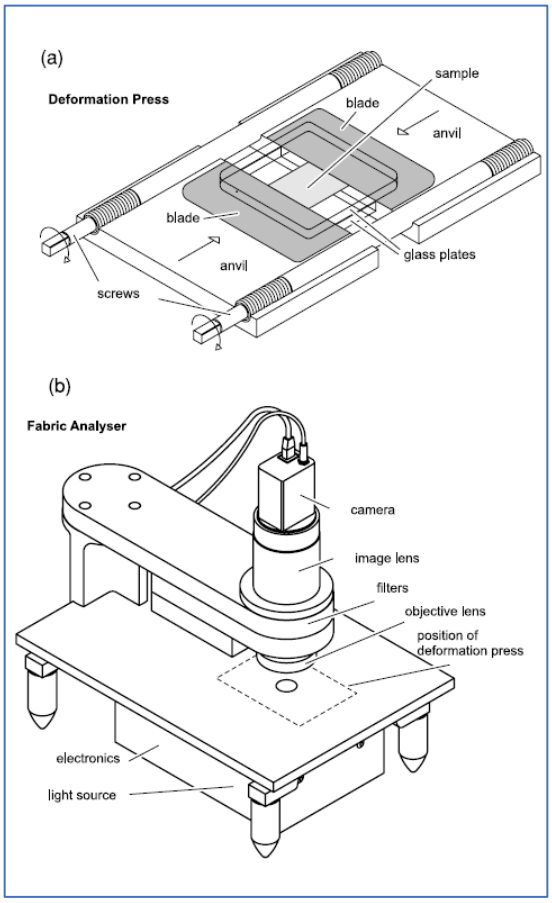

Figure 3: a) Sketch of a deformation press like the one used in the experiment. b) Sketch of the G50 Fabric Analyzer. It is an older version than the one used in this experiment, but the setup is identical.
From Peternell, Russell-Head, & Wilson, (2011)

The images depicting the sample at progressive stages of deformation was captured using a fabric analyzer microscope (G60) (Fig 3). The analyzer generates AVI format video files from a series of singe-frame measurements. Every single frame consists of several images, detailing different properties of the sample at the given moment of capture. In this experiment images detailing geometric quality,

orientation, retardation quality, retardation, flat trend and trend was produced, in addition to one plain- and one cross-polarized image of the sample per data-frame (Peternell et al., 2011). It should be noted that the only image type used in this report is the plain polarized one as this image type best distinguished the carbon dioxide bubble voids from the ice matrix.

The data was provided by Mark Peternell at the Department of Geosciences at Gothenburg University, who also conducted the experiments.

The first and final image, which show the full extent of the sample were captured at a resolution of 50,0 mm wide and 30,0 mm high with a pixel resolution of 100 pixels per mm. All intermediate stages of deformation were recorded as 20x20 mm images, centered on the middle of the thin section, with a 100 pixel per mm ratio.

2.2 Analysis

2.2.1 Strain analysis

The strain was calculated by measuring the lengths of the samples before ($Length_{initial}$) and after ($Length_{final}$) deformation:

$$Equation\ 1:\quad Strain_{total} = \frac{Length_{final} - Lenght_{initial}}{Length_{initial}}$$

The lengths were measured by loading the images into Microsoft Paint and tracing the edges of the samples. By cropping the image, the width and height of the sample were recorded in pixels. The measurements were then converted to millimeters by dividing the number of pixels by the ratio of pixels to millimeters in each image.

2.2.2 Analyzing progressive deformation

The progressive deformation was measured by calculating the projected strain ellipse of each data frame. Two methods were used to track the progressive deformation: The Fry method and the R_f/Φ method, the theory of which are outlined above. All measured ellipses and center points needed for the measurements were produced by tracing the bubbles in the EllipseFit freeware software (Vollmer, 2018) using the tools *Shape* and *Filled shape* as appropriate. In order to analyze the full deformation process, the initial and final frames were cropped to images of 20x20 millimeters, centered on the same are as the intermediate data-frames. Care was taken to not include any bubbles which could not be measured in all fourteen data frames as well as to remove any obvious outliers.

There are black rings present in roughly 40 % of the air bubble voids. These rings are the result of air trapped between the sample and the overlying glass plate used to contain the sample during deformation. These air bubbles are surrounded by silicone oil. It is the oil that causes the black rings to appear. Where present, these air pockets may obscure boundaries of the voids which makes some bubbles unusable. When digitalizing the bubble markers, many boundaries were covered by black rings, but the coverage was deemed small enough to approximate the shape of the bubble.

The strain ellipse of each data frame was calculated digitally using algorithms integrated in the EllipseFit software. The strain ellipse derived from the R_f/Φ method was calculated using the eigenvector algorithm proposed by Toshihiko Shimamoto and Yukio Ikeda (Shimamoto & Ikeda, 1976). The strain ellipse derived from the Fry method was calculated using a *point density contrast* Void fit function proposed by John W.F. Waldron and K.D. Wallace *(Waldron & Wallace, 2007).*

The strain ellipses derived from the EllipseFit software was then used to calculate the total and incremental strain imposed on the sample throughout the deformation process. As the type of strain

imposed on the sample was compressional the effective strain was measured as the short axis divided by the long axis:

Equation 2: $\frac{R_{(\text{short axis})}}{R_{(\text{Long axis})}} = \frac{1}{Rs} = Rs^{-1} = \text{The strain in the sample as determined by the short axis}$

And the total strain was calculated by inserting the calculated strain into the equation 1:

Equation 3: $Strain_{total} = \frac{Rs^{-1}{}_{Final} - Rs^{-1}{}_{initial}}{Rs^{-1}{}_{initial}}$

where Rs(initial) corresponds to the axial ratio of the strain ellipsis found by analyzing the initial image and Rs(Final) corresponds to the axial ratio of the strain ellipsis found by analyzing the final image.

To find the incremental strain imposed on the sample at different stages the initial axial ratio was supplemented by the ratio corresponding to the previous frame and the final axial ratio was supplemented with the axial ratio for the stage which was being analyzed:

Equation 4: $Strain_{Incremental(X)} = \frac{Rs^{-1}{}_{(X)} - Rs^{-1}{}_{(X-1)}}{Rs^{-1}{}_{(X-1)}} =$

$The\ strain\ imposed\ between\ frame\ number\ X\ and\ X-1$

where X equals the number corresponding to the frame being analyzed.

The incremental strain derived from the manual strain measurement is calculated by assuming a constant strain rate. This is done by dividing the final strain over the number of stages, minus the initial stage, as we know that no strain has been imposed on the sample in the initial stage.

2.2.3 Robustness analysis

An analysis was made to see at what amount of data points the results started deviating significantly from the results found in this report. The purpose of this analysis was to find the minimum amount of data points the students need to produce per data frame when analyzing the samples. One set of data obtained from a data frame representing the halfway point of deformation was chosen for this analysis. The sample strain ellipsis R- and Φ-value was calculated at a varying amount of data points, starting at an initial sample size of 85 data points. The sample size was progressively reduced by removing five random data points per calculation and this procedure was repeated seven times, yielding seven series. The values obtained from the Rf/Φ method and the Fry method was plotted separately.

The maximum acceptable deviation of the R-value was arbitrarily set to 5% above and below the results obtained with 85 data points. The maximum acceptable deviation of the Φ-value was arbitrarily set to 5 degrees above and below the results obtained with 85 data points.

2.3 Constructing the exercise

The exercise was constructed in two parts, one which is fully manual and one which uses the EllipseFit software.

2.3.1 Manual exercise

The manual exercise was constructed to teach students how the methods work. It was written as a document using Microsoft word, with tables constructed in the same software. Three images, depicting the initial, an intermediate and the final stage of deformation were used as the material on which the students will do manual measurements. Two tables and two cartesian plots were drawn for the students to work with during the exercise (supplementary data 1).

2.3.2 Computer exercise

The purpose of the exercise was to teach students how to do practical structural analysis. As such it is closely related to the analysis section of this report, using the same data.

Written instructions were produced to teach the students to navigate the software. These instructions were written in a tutorial format, utilizing one data frame from the thin section experiment and data produced in the analysis section of this report.

In order to streamline the student's results a reference image with recommended markers which to trace and analyze were produced and included in the data supplied to the students. An excel spreadsheet with premade, blank tables and images showing the appropriate markers which should be used were produced as well to guide the student's analysis (supplementary data 2).

3 Results

3.1 Air bubble textures and deformation features

The deformation process was completed in 64 hours and 30 minutes, which is equal to 3870 minutes. The total strain was measured to be -0.216, or -21,6% over the entire deformation process. The negative sign before the strain value indicates a compressional strain.

In the initial state, before the deformation has started, the orientations of the bubbles major axis are essentially randomly orientated. When summed and averaged the mean orientation of the bubbles long axis is at an angle negative 27.3 degrees from the horizontal axis of the sample (Fig 4).

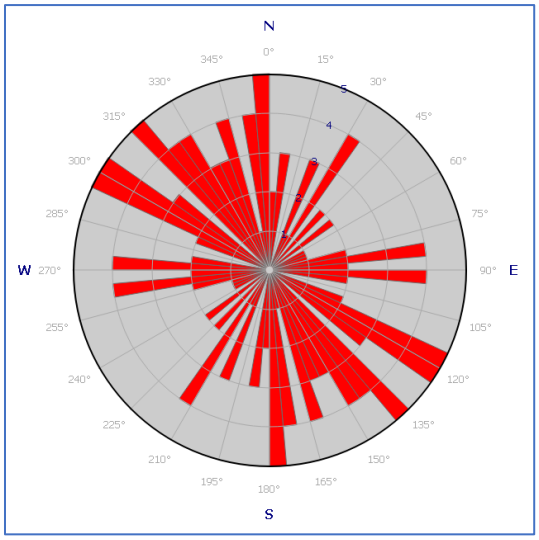

Figure 4: a polar plot showing the orientation of the bubble's major axis in the initial state of the sample. The red dot represents the average orientation of all bubble long axis.

Throughout the sample most bubbles lose their initial symmetry and become distorted along the grain boundaries of neighboring ice crystals. During the deformation process some of the voids are broken up into smaller individual bubbles. The ice crystals do not change shape at an equal rate to that of the change of the air bubbles. All these features of deformation are presented in Figure 5. While this figure does present an extreme case, it should be noted that most bubble voids present in the sample show some similar distortion in the final stages. The borders of the voids in Figure 6, which shows the full extent of the sample in the initial stages, show them to be rounded. There appears to be little interference on the shape of the voids from the surrounding crystal matrix. In Figure 7, which shows the full extent of the sample in the final stage of deformation, the borders of the voids are no longer rounded. At this stage most borders are irregular and indented by the surrounding crystals.

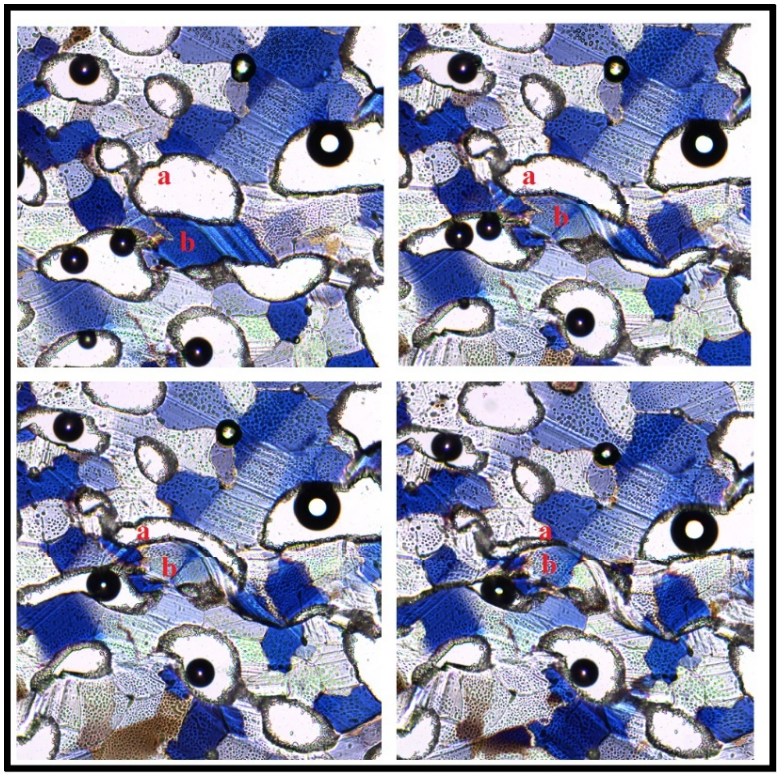

Figure 5: The distortion and subsequent division of an air bubble during the late stages of deformation. The black rings are a result of trapped air surrounded by silicone oil. a) An air-bubble. b) A crystal of ice around which an air bubble is being deformed.

There is a gap in between the top part of the ice sample and the metal arm in the initial state as can be seen in Figure 6.

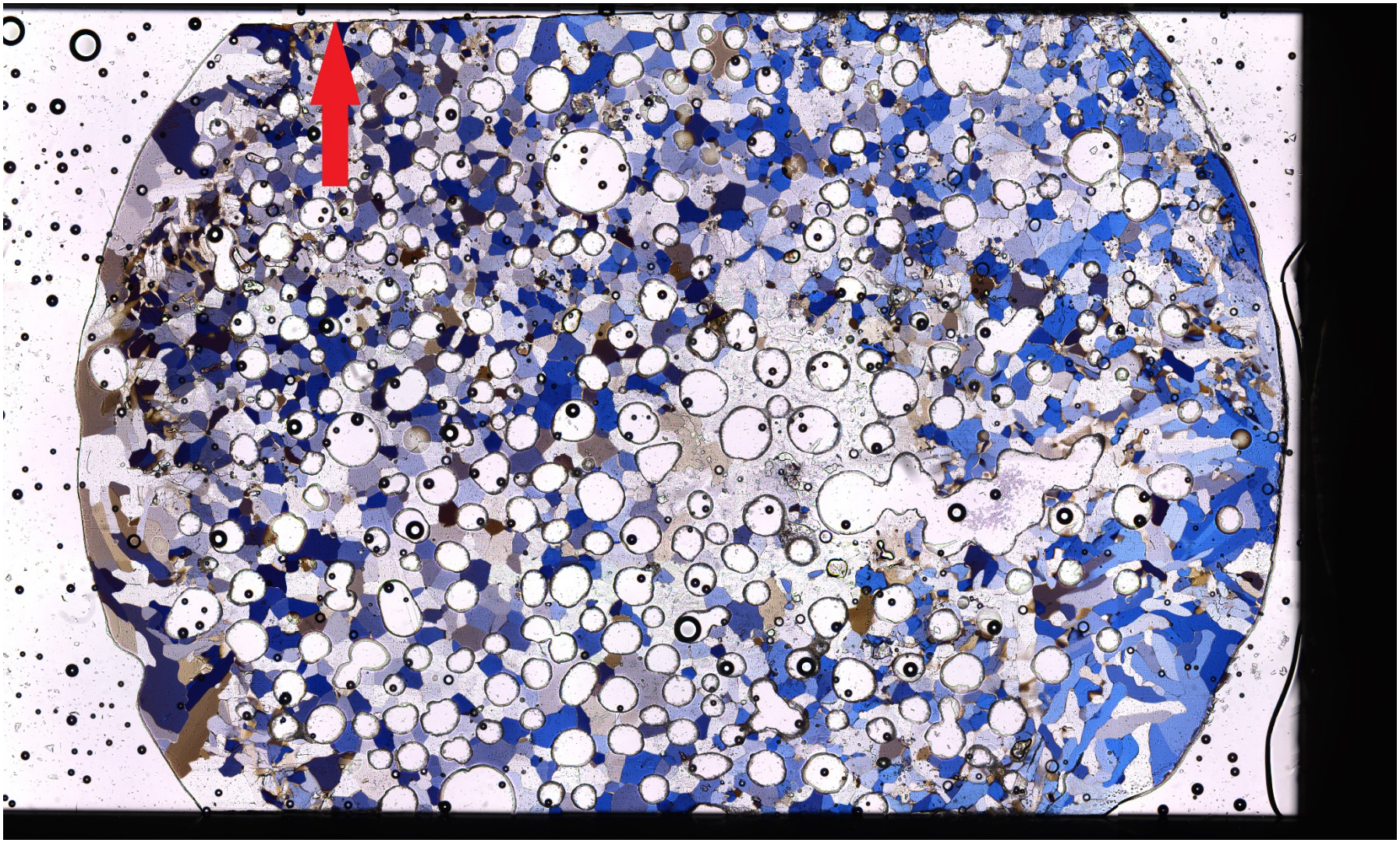

Figure 6: The initial state of the ice thin section. The black bars on the top and the bottom are the metal arms which hold the thin section and applies pressure on it. The total breadth of the sample measures 28,78 mm, as measured from the top contact between ice and metal to the bottom contact between ice and metal. The red arrow indicates a gap between the ice and the upper metal arm.

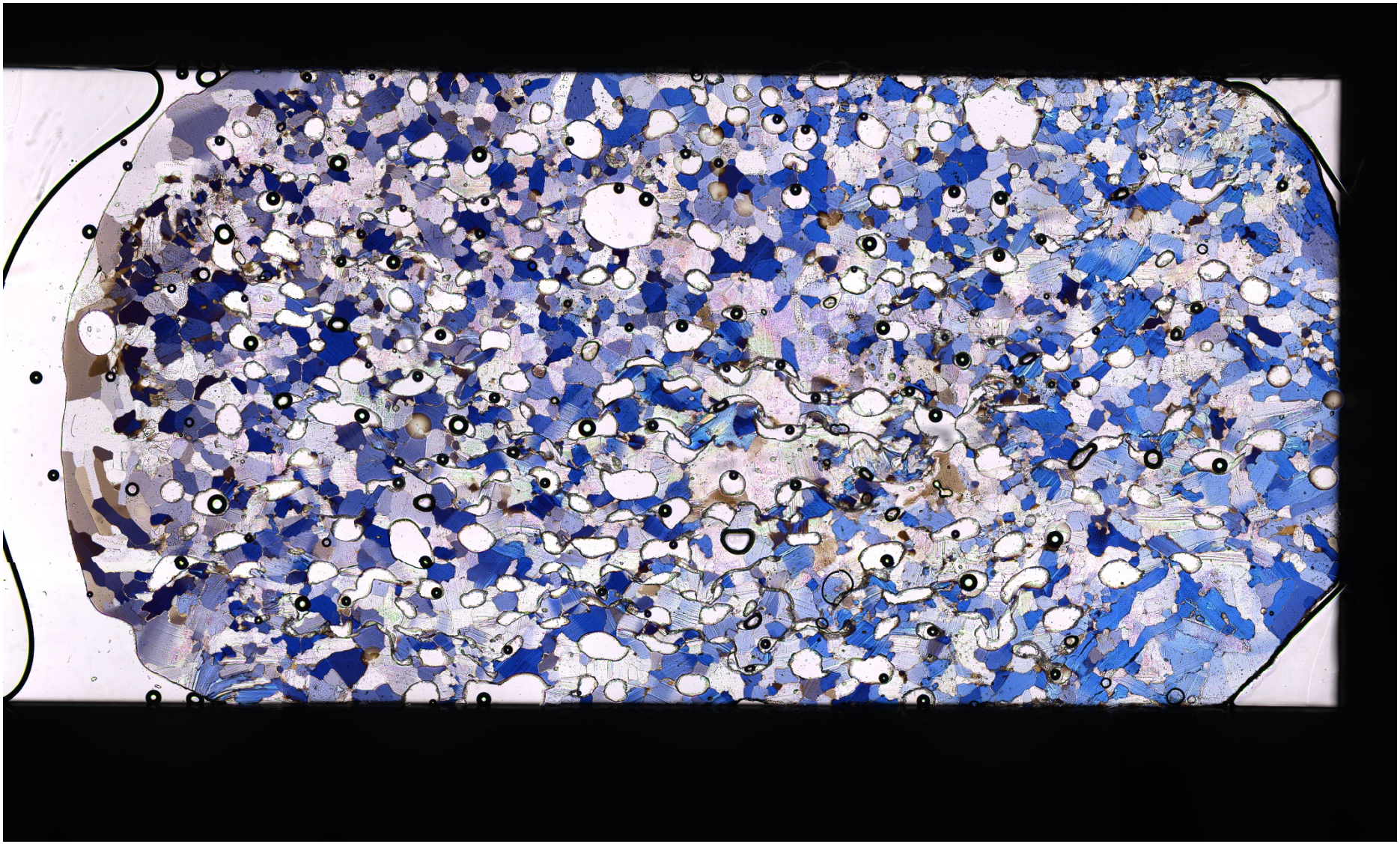

Figure 7: the final state of the ice thin section. The black bars on the top and the bottom are the metal arms which hold the thin section and applies pressure on it. The total breadth of the sample measures 22,55 mm, as measured from the top contact between ice and metal to the bottom contact between ice and metal

3.2 Digitalization

The carbon dioxide bubbles used as markers in the ice matrix were successfully traced in the EllipseFit software. About forty percent of the bubble inclusions were overlaid by gaseous inclusions which obscured the borders of the bubble-ice contacts. This means that some borders had to be approximated and that some markers were fully unusable. For every 20x20mm data frame an average of 115 markers were able to be digitized, out of which 99 markers were able to be tracked through all data frames. Eliminating outliers and bubbles which fractured into two minor bubbles during deformation yielded a sample of 82 bubbles which could be tracked through all data frames.

Example data frames with their corresponding maps of digitized ellipses are presented in Figure 8.

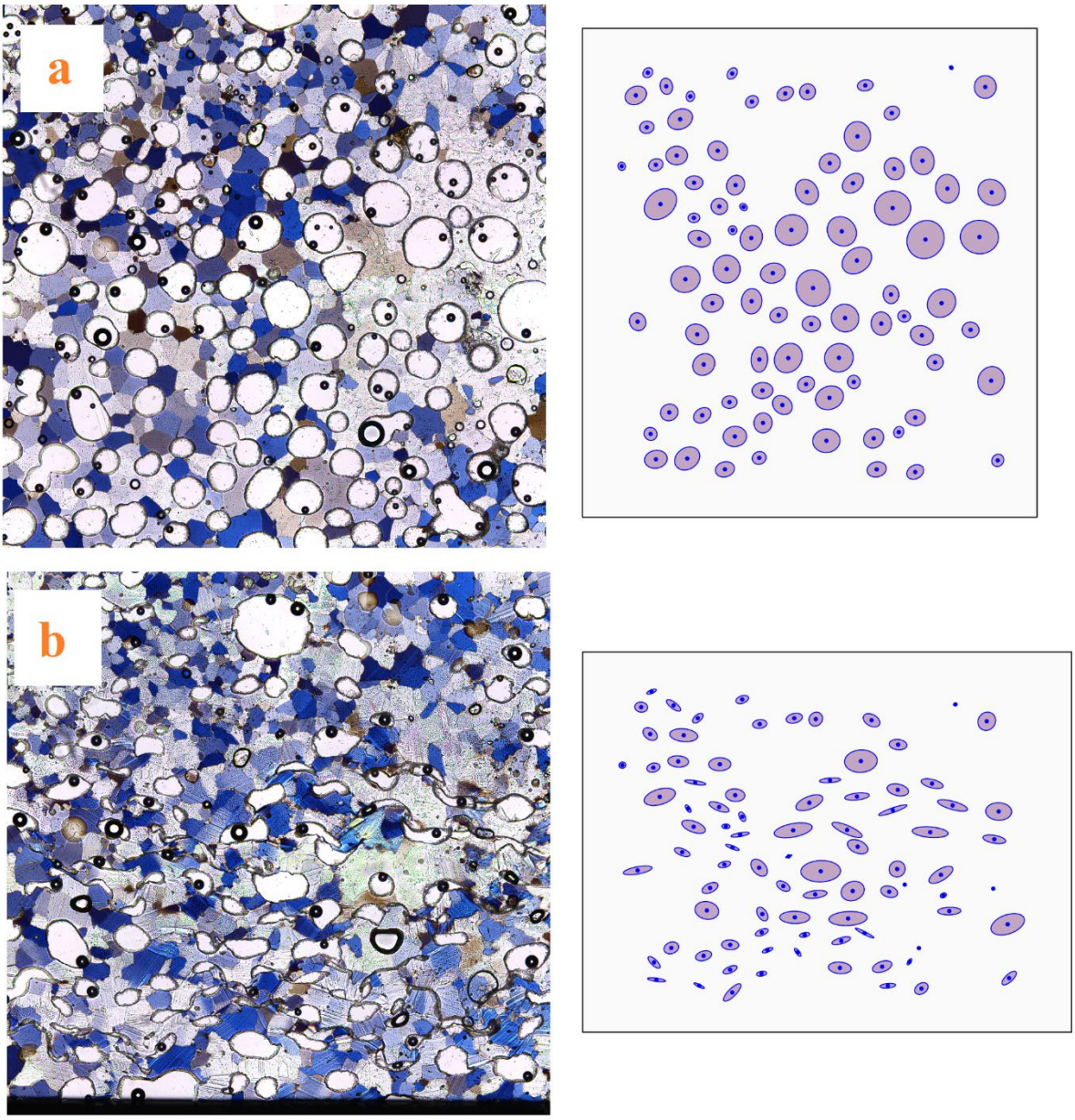

Figure 8: Example data frames (microphotograph) and their corresponding strain maps with ellipses projected from strain markers. a) the initial state of the sample. b) the state of the sample after a completed deformation process.

3.3 Strain analysis

The results of strain analysis using both the R_f/Φ method and the fry method are presented in Table 1. The data refers to the properties of the projected strain ellipsis, as well as the calculated incremental strain imposed on the sample between the analyzed stage and the one before it. The results of the manually measured strain is also included. The ellipse data is derived from the R_f/Φ method and the point data is derived from the Fry method.

Table 1: The results from digital analysis. Ellipse data was analyzed using the R_f/Φ method. Point data was analyzed using the Fry method.

Sample nr	Elapsed time (minutes)	Strain from manual measurement	Strain from Ellipse data	Strain from Point data	Ellipse data Axial ratio	Point data Axial ratio	Ellipse data Major axis orientation (degrees)	Point data Major axis orientation (degrees)
1	0	0,0%	0,0%	0,0%	1,05	1,08	-39,60	-42,90
2	40	-0,2%	-0,8%	1,4%	1,06	1,06	-26,80	-57,00
3	310	-1,7%	-1,0%	1,6%	1,06	1,06	-23,50	-35,00
4	610	-3,3%	-4,2%	0,9%	1,09	1,07	-11,20	-20,50
5	910	-5,0%	-7,4%	-7,7%	1,13	1,17	-8,60	-10,50
6	1210	-6,6%	-11,4%	-6,0%	1,18	1,15	-7,30	-4,60
7	1510	-8,3%	-15,7%	-13,2%	1,24	1,24	-6,80	-4,50
8	1810	-9,9%	-19,8%	-16,4%	1,31	1,28	-3,90	-0,30
9	2110	-11,5%	-24,4%	-21,5%	1,39	1,35	-4,00	-0,60
10	2410	-11,5%	-28,2%	-24,1%	1,46	1,39	-4,00	3,10
11	2710	-13,2%	-30,2%	-22,2%	1,50	1,36	-3,60	8,50
12	3010	-14,8%	-33,3%	-31,4%	1,57	1,50	-1,70	9,10
13	3310	-18,1%	-36,1%	-33,3%	1,64	1,53	-1,20	10,50
14	3610	-19,7%	-38,4%	-33,0%	1,70	1,52	-1,20	13,30
15	3910	-21,4%	-38,8%	-38,2%	1,71	1,61	-0,10	13,10
16	3960	-21,6%	-39,6%	-38,2%	1,74	1,61	-0,80	12,00
Total Change	3960	-21,6%	-39,6%	-38,2%	0,69	0,53	38,85	54,82

The imposed strain calculated from the digital analysis is proportional to the increased ellipticity of the strain ellipsis. Note that the axis corresponding to the increase in strain is inverted in the plot representing the accumulated strain over time (fig 9). As the strain is compressional, the strain is negative, meaning that a lower value indicates a higher degree of strain imposed on the sample. Note that the time between the capture of the initial and the second image used in this analysis is comparatively short relative to the rest of the series: only 40 minutes. The same is true for the time between the second to last image and the final image with 60 minutes between them. The average time between all other frames is 300 minutes.

The trends derived from the digital analysis does not indicate a perfect linear trend. In the beginning phase, from the first stage to the fourth the R_f/Φ method indicate low incremental strains between the stages (fig 9). The fry method indicates that the degree of strain was lowered between stage one, two, three and four. After stage four the strain rate is increased. The data derived from the R_f/Φ method indicates that the strain was linear after this point. The Fry method indicates a similar trend, where the calculated strain start increasing rapidly after the fourth image, however, the trend is not as smooth as the one representing the values derived from the ellipse data. Deviations from the linear trend appear in the data from Image five and image eleven (Fig 9).

Both the Fry and the R_f/Φ method yield a higher calculated final strain than the strain derived from the manual measurement of the sample. The results from the Fry method indicate a 16,5% higher final strain than the measured final strain and the R_f/Φ method indicate a 18,0% higher final strain.

The final orientation of the strain ellipse derived from the Fry and the R_f/Φ method differ by 11,2 degrees. The ellipse data indicate that the final orientation is 0,8 degrees from the horizontal axis of the sample, which means it is parallel to the assumed strain X direction. The point data indicate a 12-degree deviation from the horizontal axis of the sample, which indicates that the maximum strain direction of the digitalized markers is not aligned with the assumed strain X direction.

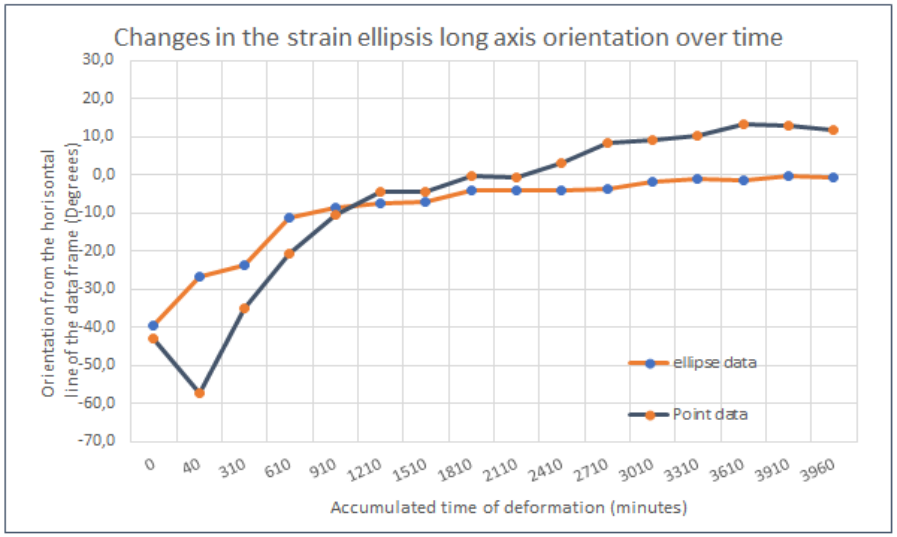

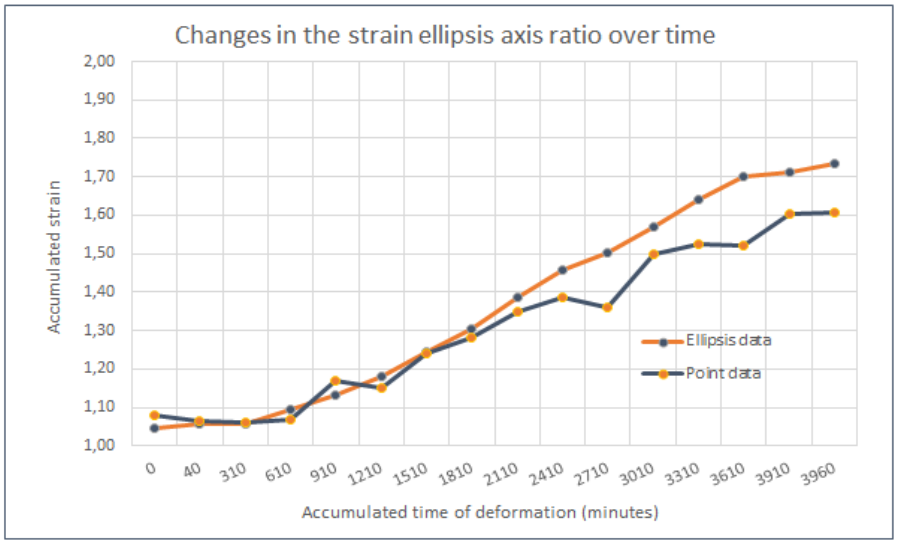

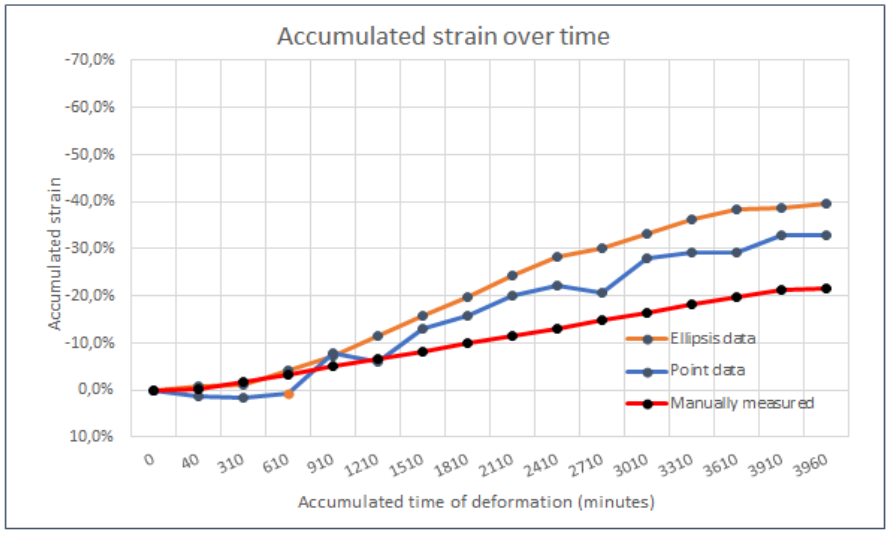

Figure 9: Plots representing the changes in long axis orientation, Strain ellipsis ratio and the accumulated strain over time as calculated using the Ellipse fit software.

3.4 Robustness analysis

The results are presented visually in Figure 9.

The first deviation outside of the acceptable range appear at a sample size of 45 in the R-value derived from R_f/Φ analysis. At a sample size of 40 two series has deviated outside of acceptable bounds. The first major deviation occurs at a sample size of 30 data points and at progressively lower amounts below this sample size the data series truly start to break up and scatter about the mean. The Φ-value plot shows similar trends with the first deviation outside of acceptable bounds occurring at a sample size of 30 data points.

The plots derived by using the Fry method proves to be less resistant to the reduction of sample size than the plots derived from the R_f/Φ, with the first minor deviation on the R-plot occurring at 80 data points, which is at the first stage of data point removal. A deviation which equals the first major deviation in the R_f/Φ derived plot occurs as 75 data points remain, which is at the second stage of data point removal (fig 9). The trends do not recover from this point and values deviating up to 230% from the value calculated at full sample size are recorded. The Φ-value plot derived from the Fry method show similar trends to the R-value plot derived from the Fry method. The first major deviation occurs as 80 data points remain.

3.5 Student exercises

The student exercises resulting from this experiment accompany this report as separate documents.

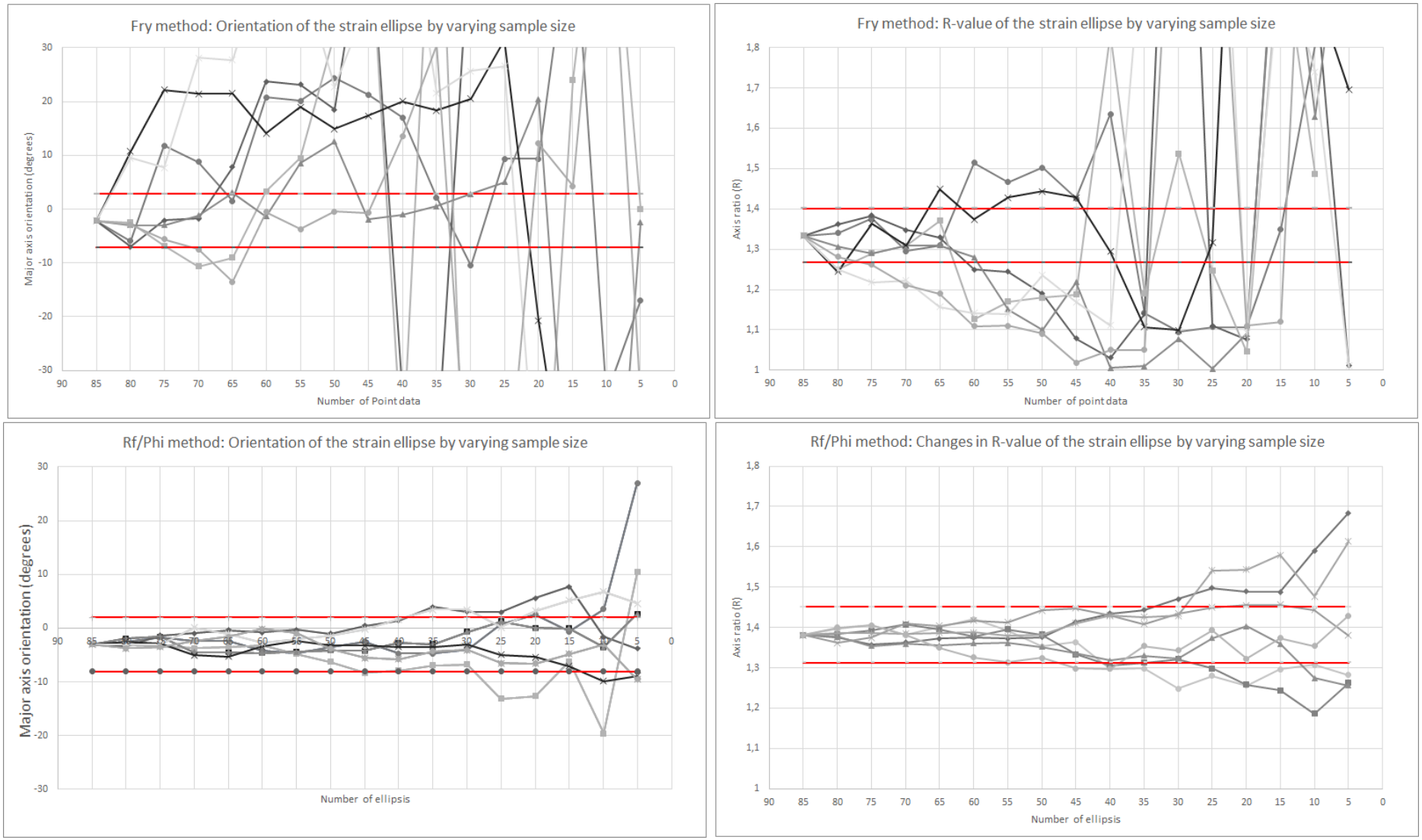

Figure 10: Results from the robustness analysis. The red lines indicate the maximum and minimum acceptable values. The monochrome series are representing the results of the calculations with progressively fewer data poi

4 Discussion

4.1 The use of carbon dioxide bubbles in ice as strain markers.

From the results we see that the carbon dioxide bubbles are functional markers and are useable for tracking the incremental strain the sample has been subjected to. Enough bubbles are free enough from obscurity imposed by the silicone oil rings and intact enough to be tracked trough the deformation process for us to be able to use them in a strain analysis.

The ability to track a good number of strain markers from the beginning to the end of the process means that the incremental strain is measureable throughout the series. This fact in itself is enough to deem the experiment a success. In addition, a plain polarized image of the bubbles (Fig 6 and 7) allow the bubbles to be digitalized and measured as they are easily distinguishable from the ice matrix.

The air bubbles ringed with silicone oil appear to prefer to cluster in the carbon dioxide bubble voids. As such, the lubricating silicone oil used in the sample deformation experiment, while instrumental in reducing the friction between the glass and the ice sample during the deformation process (C. Wilson, 1986), does obscure many of the bubble outlines.

4.2 Applying the strain analysis methods

The incremental strain, while increasing at a high ratio and resulting in a high final value, is fully trackable throughout the series which was the goal of the experiment. The higher results from the computer analysis may be the result of several factors.

First off, The R_f/Φ method yield a higher final strain than the Fry method. A probable cause is that the R_f/Φ method is much more dependent of the geometry of the bubbles than the Fry method. As seen when studying figure 6 and 7 closely, the bubbles are prone to losing their symmetry. This feature may be a result of some difference in the properties of the ice and the carbon dioxide bubble voids. The bubbles are weaker in some regard to the ice and many will deform and shatter when pressed by the ice rather than align with the movement of the ice matrix. If this relationship causes the bubbles to contract and have their shapes changed more easily than the surrounding ice matrix then the increased ellipticity of these bubbles should not equal the contraction of the sample as a whole. It should rather be higher as the bubbles deform more easily during the deformation, which increases their final R-values and as such the strain indicated from the ellipses. The Fry method on the other hand does only derive its values from the center points of the markers, which does not appear to change as much as the ellipticity of the objects when they are deformed.

Another thing to consider is that the subsection of the sample which is being analyzed is centered on the center of the sample. As the sample is compressed the matrix will be preferentially deformed in the middle, creating a center line of maximum deformation. Because the sample of markers used in this analysis are taken from the center portion of the sample, they will probably record a higher strain than the full scale of the ice thin section.

The result tells us that the orientation of the final strain ellipse differs between the used analysis methods. One reason for this is that the Fry method tracks the movement of the markers rather than their change in shape. In the analyzed section of the sample there may be a movement of the ice equal to the orientation the Fry method indicates. If this is true, the R_f/Φ method does not seem to follow the local change in orientation. This could be because the bubbles will rather disintegrate and give way for the ice than change direction along with the ice crystal matrix.

In the initial stage there is a gap between the sample and the metal arm which applies pressure on it during the deformation process (fig 6). This may explain the initially lower strain rate I found in the initial stages of the deformation process (fig 9).

4.3 Using the data in a student exercise

There is a clear trend towards an elongation and reorientation of the markers which matches the broad trends of the sample. From this trend, the students should be able to identify the basic features of the type of strain present and as such it can be used in a student exercise. There is no need for a high degree of certainty in the results in order to make a good material for a student exercise. On the contrary, when the material has a measurable degree of error, as this material has, this error may be used to evaluate the techniques used.

The robustness analysis indicates that a sample of 45 markers should be enough to apply the R_f/Φ method. As such this is the minimum limit set for the manual exercises where students are asked to find the properties of a sample using this method. Problems arise when using the Fry method in the manual exercise. The data deviates significantly below 80 datapoints, yet 80 datapoints is a very high number to expect students to use. A compromise may have to be made.

When using the data for a computer exercise the digitalization of the marker bubbles yield elliptical data and point data at the same time. For this reason, there is no motive for why the data series should contain less than the full 82 points data used as the basis for the analysis presented in this report.

4.4 Advantages and disadvantages to other materials

The advantage of using ice as a material in this analysis is that we know the initial state of the sample and that we can track the deformation process in incremental stages. As the sample was created in an isolated system, we can assume that the markers are oriented in a random arrangement in the original state, as no force has been imposed on the sample during its formation. Thus, any changes in elongation and orientation resulting from the strain imposed on the sample between the initial and final stages are traceable and, under ideal circumstances, we would be able to isolate and quantify it. In other materials typically used in student exercises, such as rock samples with oolites or images of till fabrics, the samples are taken from open systems and the initial and intermediate stages of deformation are lost. In using ice, the students may follow the deformation process in situ. The analysis done in this study show that while there may be some inaccuracy tied to using air bubbles as strain markers, the overall trend of the deformation is preserved and may be tracible.

5 Conclusions

The attempt to track the incremental changes in strain of a progressively deformed ice thin section, using air bubbles as strain markers, is a great success. The overall trend of deformation may be found and analyzed yet the habit of bubble breakup and disproportionate deformation introduces error into the analysis. Despite this inherent flaw the material has some advantages over other more orthodox materials which are commonly used by students to practice the basics of strain analysis. Because the initial state and all intermediate stages of deformation may be observed the students may study strain as it develops.

Acknowledgements

I would like to thank Mark Peternell for supplying me with data and guiding me through the process of writing this report.

References

Fonte, F. A. M., & Nistal, M. L. (2018). *Methodologies and Software for Creating Audiovisual Open Educational Resources.* Paper presented at the 2018 International Symposium on Computers in Education (SIIE).

Dunnet, D. (1969). A technique of finite strain analysis using elliptical particles. *Tectonophysics, 7*(2), 117-136.

Fry, N. (1979). Random point distributions and strain measurement in rocks. *Tectonophysics, 60*(1-2), 89-105.

Lisle, R. J. (1985). *Geological Strain Analysis: A Manual for the Rf/0 Technique*: Pergamon Press.

Matthews, P., Bond, R., & Van Den Berg, J. (1974). An algebraic method of strain analysis using elliptical markers. *Tectonophysics, 24*(1-2), 31-67.

Peternell, M., Russell-Head, D., & Wilson, C. (2011). A technique for recording polycrystalline structure and orientation during in situ deformation cycles of rock analogues using an automated fabric analyser. *Journal of Microscopy, 242*(2), 181-188.

Ramsay, J. G. (1967). Folding and fracturing of rocks. *Mc Graw Hill Book Company, 568*.

Shimamoto, T., & Ikeda, Y. (1976). A simple algebraic method for strain estimation from deformed ellipsoidal objects. 1. Basic theory. *Tectonophysics, 36*(4), 315-337.

Soares, A., & Dias, R. (2015). Fry and Rf/φ strain methods constraints and fold transection mechanisms in the NW Iberian Variscides. *Journal of Structural Geology, 79*, 19-30.

Twiss, R., & Moores, E. (1992). M., 1992, Structural Geology. In: New York, WH Freeman and Company.

Waldron, J. W., & Wallace, K. (2007). Objective fitting of ellipses in the centre-to-centre (Fry) method of strain analysis. *Journal of Structural Geology, 29*(9), 1430-1444.

Wilson, C. (1986). Deformation induced recrystallization of ice: the application of in situ experiments. In *Mineral and rock deformation: Laboratory studies* (Vol. 36, pp. 213-232): Am. Geophys. Union.

Wilson, C. J. L., Peternell, M., Piazolo, S., & Luzin, V. (2012). Ice an analogue used for rock textural development. *Abstracts - Geological Society of Australia, 102*, 143.

Wilson, C. J. L., Peternell, M., Piazolo, S., & Luzin, V. (2014). Microstructure and fabric development in ice; lessons learned from in situ experiments and implications for understanding rock evolution. *Journal of Structural Geology, 61*, 50-77. doi:10.1016/j.jsg.2013.05.006

Vitale, S., & Mazzoli, S. (2005). Influence of object concentration on finite strain and effective viscosity contrast: insights from naturally deformed packstones. *Journal of Structural Geology, 27*(12), 2135-2149.

Vollmer, F. W. (2018). Automatic contouring of geologic fabric and finite strain data on the unit hyperboloid. *Computers & Geosciences, 115*, 134-142.

Yamaji, A. (2005). Finite tectonic strain and its error, as estimated from elliptical objects with a class of initial preferred orientations. *Journal of Structural Geology, 27*(11), 2030-2042.

Supplementary data 1: Tools for the manual exercise

Figure 11: Cartesian plot on which the students will plot their data in order to perform a manual Rf/Phi analysis

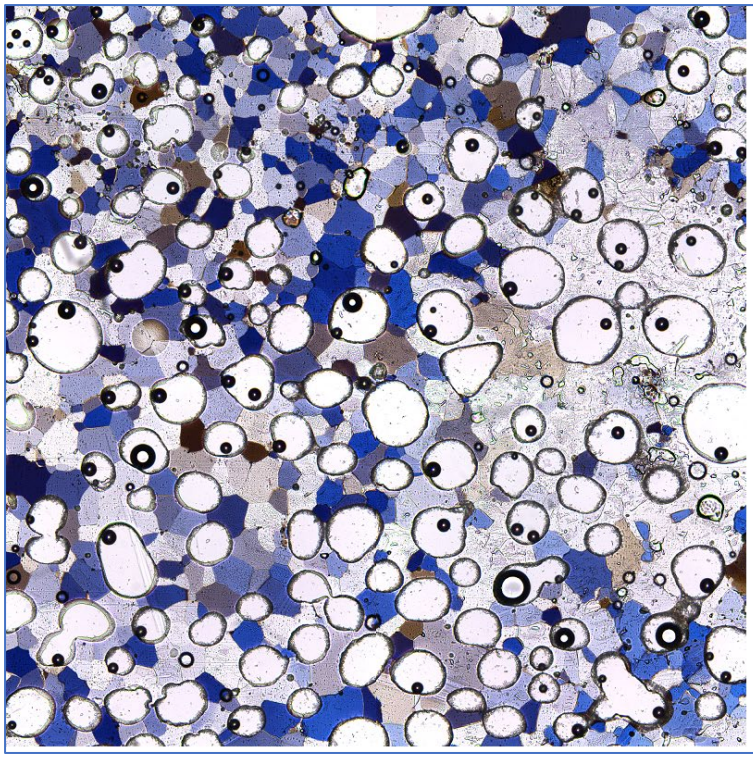

Id	Long axis (mm)	Short axis (mm)	ϕ-value (degrees)	R_f-value (Unitless)
1				
2				
3				
4				
5				
6				
7				
8				
9				
10				
11				
12				
13				
14				
15				
16				
17				
18				
19				
20				
21				
22				
23				
24				
25				
26				
27				
28				
29				
30				
31				
32				
33				
34				
35				
36				
37				
38				
39				
40				

R_{max}	
R_{min}	
R_S	
Ri	

Figure 12: An image the students will work on to perform the Rf/phi method and corresponding tables in which to write their results

Supplementary data 2: Tools for the computer exercise

	A	B	C	D	E	F	G
	Image number	time accumulative (minutes)	Rs-value from Rf/Φ-method	Φ-value from Rf/Φ-method (polar)	Φ-value from Rf/Φ-method (Cartesian)	Rs-value from Fry method	Φ-value from Fry method
	1	0			-180,0		
	4	610			-180,0		
	6	1210			-180,0		
	8	1810	A	B	-180,0	C	D
	10	2410			-180,0		
	12	3010			-180,0		
	14	3610			-180,0		
	16	3960			-180,0		
10							
11	Image number	Ellipse incremental strain	Ellipse Strain accumulative	Point incremental strain	Fry method Strain accumulative		
12	1	0%	0%	0%	0%		
13	4	#DIV/0!	#DIV/0!	#DIV/0!	#DIV/0!		
14	6	#DIV/0!	#DIV/0!	#DIV/0!	#DIV/0!		
15	8	#DIV/0!	#DIV/0!	#DIV/0!	#DIV/0!		
16	10	#DIV/0!	#DIV/0!	#DIV/0!	#DIV/0!		
17	12	#DIV/0!	#DIV/0!	#DIV/0!	#DIV/0!		
18	14	#DIV/0!	#DIV/0!	#DIV/0!	#DIV/0!		
19	16	#DIV/0!	#DIV/0!	#DIV/0!	#DIV/0!		

Figure 43: An excel sheet which is provided to the students in order to easier plot their data. The ellipsis data is pasted into column A and B. Point data is plotted into C and D. The strain is calculated automatically once the strain ellipse Axial ratios are plotted.

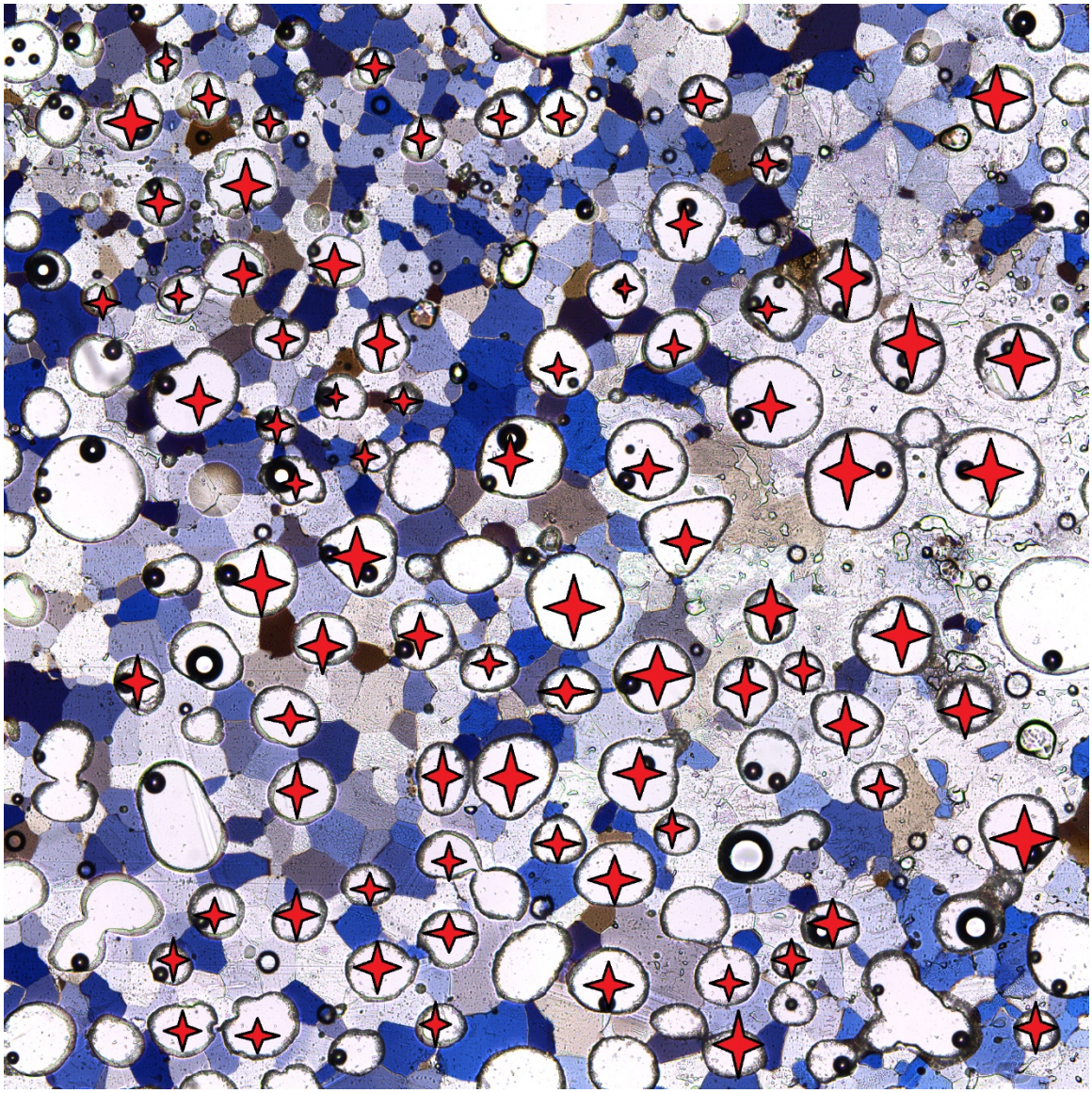

Figure 54: An example image showing the bubbles which are recommended for analysis.